

Article

Deactivation Effect of CaO on Mn-Ce/AC Catalyst for SCR of NO with NH₃ at Low Temperature

Zenghui Su, Shan Ren ^{*}, Zhichao Chen, Jie Yang, Yuhan Zhou, Lijun Jiang and Chen Yang

College of Materials Science and Engineering, Chongqing University, Chongqing 400044, China; suzenghui@cqu.edu.cn (Z.S.); C.ZhiChao@cqu.edu.cn (Z.C.); jie.yang@cqu.edu.cn (J.Y.); zhouyuhan@cqu.edu.cn (Y.Z.); Jiang.Li@cqu.edu.cn (L.J.); chen.yang@cqu.edu.cn (C.Y.)

^{*} Correspondence: shan.ren@cqu.edu.cn

Received: 6 July 2020; Accepted: 1 August 2020; Published: 4 August 2020



Abstract: In this study, the poisoning effect of CaO on activated carbon (AC)-based Mn-Ce catalysts was discussed. Loading CaO inhibited the catalytic activity of the catalyst and the NO conversion of the catalyst decreased from 69.5% to 38.2% at 75 °C. The amount of MnO₂ in AC surface decreased in the process of loading CaO, which was detrimental to the Selective Catalytic Reduction (SCR) performance of the catalyst. The change of manganese oxide form inhibited generation rate for the chemisorption oxygen and NO₂, which was the most critical reason for the decrease of catalytic activity. Besides, loaded CaO entered into the pores of the catalyst, which led to the blockage of the pores and further resulted in the decrease of the Brunauer-Emmett-Teller (BET) surface area and total pore volume. It also destroyed the oxygen-containing functional groups and acid site on the surface of AC. All of these caused the deactivation of Mn-Ce/AC catalyst after loading CaO.

Keywords: CaO poisoning; Mn-Ce/AC catalyst; low-temperature SCR; less MnO₂

1. Introduction

Nitrogen oxides (NO_x) emissions from the steel plant, especially the sintering process, have contributed to local air pollution and the global environmental problems [1–3]. Many scholars believed that Selective Catalytic Reduction (SCR) of NO_x with NH₃ was the most feasible technique to solve the problem of NO_x emission in steel plant [4,5]. The operating temperature window of commercial SCR catalyst V₂O₅-WO₃/TiO₂ was about 300–400 °C [3], so it would have a sharp drop in the SCR activity when working in the sintering flue gas (120–180 °C). Therefore, the exploitation of SCR catalysts that could work well at low temperature was the primary task to solve NO_x emissions in steel plants. An attractive alternative for lower temperatures, and thus for tail-end configuration without or with much lower flue gas heating, is the application of activated carbons (ACs) [6–8]. In our previous study [1,9–12], MnO₂ and CeO₂ supported on AC catalyst showed outstanding SCR activity at the lower temperature. Therefore, it is expected to work successfully in the NO removal of sintered flue gas.

The SCR activity of the SCR catalyst was affected not only by the type of active component, but also by the damaging metal elements (K, Pb, Ca, As and Na, etc.) in the sintering flue gas. Although the Mn-Ce/AC catalyst exhibited outstanding NO conversion under ideal experimental conditions, complex flue gas conditions must be considered when the catalyst is used in the industry. Therefore, the poisoning effects of different metal elements on the catalyst should be studied systematically. In our earlier work [1], K⁺ occupied the oxygen vacancy of the catalyst, and KCl interacted with functional groups on the surface of AC, resulting in reduced adsorption of NH₃ and NO. Loaded As₂O₃ was converted to As₂O₅ preferentially by the chemisorption oxygen, which led to the decrease of the chemisorption oxygen participating in the SCR reaction [1]. The PbO poisoning over Mn-Ce/AC

catalyst was also studied by the authors [13], the result indicated that the “fast SCR” reaction was inhibited for the catalyst and caused the decrease of SCR performance.

The presence of Ca in the form of CaO, CaCl₂ or CaOH would affect the activity of commercial catalysts and TiO₂-based catalysts in flue gas, and the poisoning effect of calcium has been studied by some scholars [14–17]. Li found that the SCR performance of Ca-poisoning V₂O₅-WO₃/TiO₂ catalyst decreased seriously [14]. The poisoning effect of Ca(OH)₂ on Mn-Ce/TiO₂ catalyst was more serious compared with that of CaCl₂ [15]. The study of Liu [16] suggested that NH₃ adsorption and NO oxidation for Ce/TiO₂ were inhibited after loading CaO. Nevertheless, the behavior and effect of CaO over Mn-Ce/AC catalyst has not been researched. Therefore, the Mn-Ce/AC and CaO poisoning catalyst were prepared by in this study, aiming to investigate the deactivation reason of Mn-Ce/AC catalyst after loading CaO by a series of characterization methods.

2. Results

2.1. Catalyst Performance

Figure 1a compares the deNO_x activity of Mn-Ce/AC and CaO poisoning catalyst. Mn-Ce/AC catalyst achieved a high NO conversion of 69.4% at 75 °C, which may be mainly attributed to the NO adsorption capacity of AC. Mn-Ce/AC catalyst showed excellent SCR activity with the highest NO conversion of 96.5% at 225 °C. However, the SCR performance of the catalyst took place a noticeable change after doping CaO. The NO conversion of CaO poisoning catalyst decreased to 84.4% at 225 °C, which indicated that CaO on the AC surface inhibited the catalytic action of the Active components on AC. Noteworthily, the NO conversion was significantly decreased due to the load of CaO in the low temperature range of 75–125 °C. With the increase of temperature, the deactivation degree of CaO poisoning catalyst decreased. N₂ selectivity and N₂O concentration of the two catalysts are also displayed in Figure 1b. From Figure 1b, The N₂ selectivity of all catalyst samples decreased as the temperature increased. CaO poisoning catalyst had the smaller N₂ selectivity compared with Mn-Ce/AC catalyst. Therefore, loading CaO was unfavorable for keeping high N₂ selectivity of the catalyst. Besides, More N₂O was produced on the Mn-Ce/AC catalyst after loading CaO, which was a key factor in the decrease of N₂ selectivity for CaO poisoning catalyst.

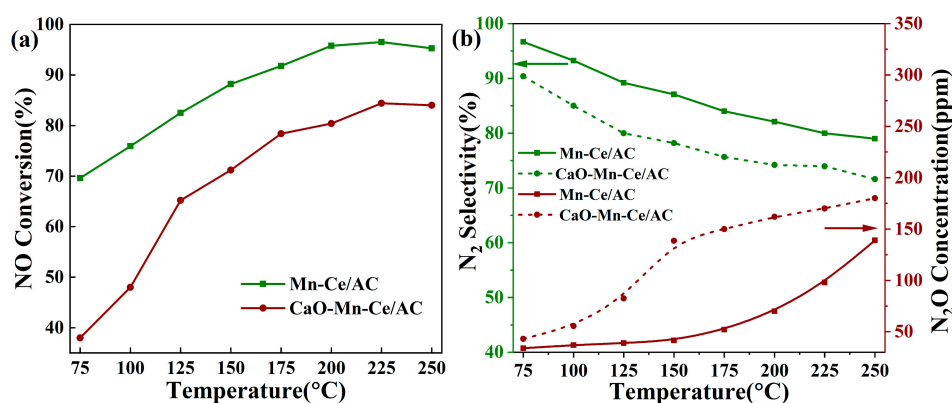


Figure 1. (a) NO conversion, (b) N₂ selectivity and N₂O concentration of the two catalysts.

2.2. Pore Properties Analysis

The pore properties of the Mn-Ce/AC and CaO poisoning catalyst are given in Table 1. It could be found from Figure 2 that the nitrogen adsorption-desorption isotherms of all catalysts were of typical type IV, with a hysteresis loop of type H4. It was a typical mesoporous material and the loading of CaO did not change the pore structure of the catalyst. Brunauer-Emmett-Teller (BET) results showed that Mn-Ce/AC catalyst had a relatively large BET surface area. The specific surface area of Mn-Ce/AC catalyst was 825 m²/g, while that of CaO poisoning catalyst was 724 m²/g. In addition, the total pore

volume decreased significantly to $0.16 \text{ cm}^3/\text{g}$ after loading CaO. However, the average pore diameter of CaO poisoning catalyst had little change. These changes may be caused by the blockage of some micropores on AC surface. Loaded CaO entered into the pores of the catalyst, which resulted in the blockage of the pores and further led to the reduction of the BET surface area and total pore volume of the catalyst.

Table 1. The textural properties of the two catalysts.

Samples	BET Surface Area (m^2/g)	Total Pore Volume (cm^3/g)	Average Pore Diameter (nm)
Mn-Ce/AC	825	0.38	4.04
CaO-Mn-Ce/AC	724	0.16	4.03

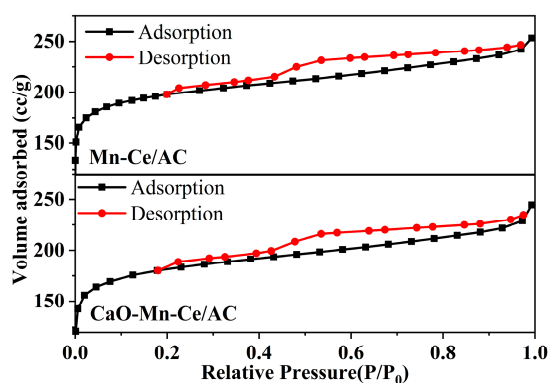


Figure 2. N_2 adsorption-desorption isotherm of the two catalysts.

2.3. SEM Analysis

To verify the conclusion of BET, the SEM characterization was performed and the surface morphology of the two catalysts is shown in Figure 3. Figure 3a is the scanning electron microscope morphology of the Mn-Ce/AC catalyst. Mn-Ce/AC catalyst had developed pores, large pore size and fine particles on the AC surface, which was consistent with the BET experimental results (Table 1). The surface of the catalyst became compacted and the total pore diameter and the number of micropores became smaller after loading CaO, because the loaded CaO entered into the pores of the catalyst, which led to the blockage of the pores and further led to the destruction of carbon pore morphology of AC, and the surface of the catalyst became rough. Poor surface morphology would hinder the adsorption behavior of reacted gas.

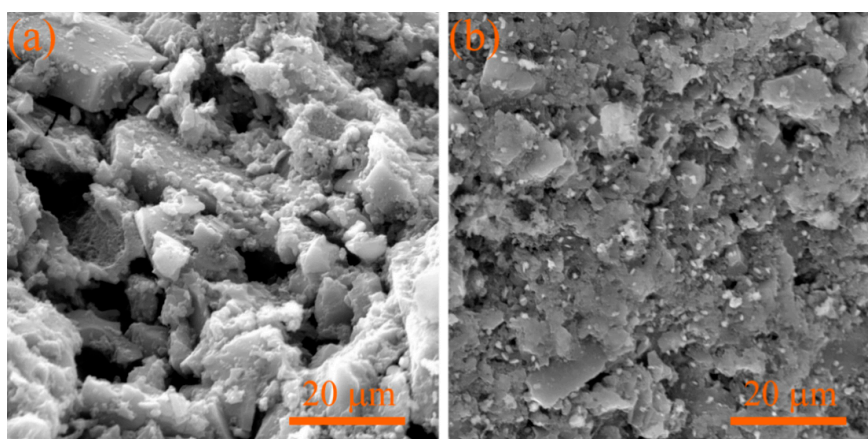


Figure 3. Surface morphology of (a) Mn-Ce/AC; (b) CaO-Mn-Ce/AC.

2.4. XRD Analysis

Figure 4 displays the XRD patterns of Mn-Ce/AC and CaO poisoning catalyst. From Figure 4, both catalysts appeared the broad diffraction peaks of graphite crystallite with layer structure (002) at 22–31° and turbostratic graphite-like structure (100) at 41–47° [18,19]. In the XRD curves of Mn-Ce/AC, the characteristic peaks of SiO₂ at 26.65° and the weak diffraction peak of CeO₂ (JCPDS 42-1348) at 35.5° were detected [13,20]. However, there were three new characteristic peaks of 2θ = 36.79°, 50.34° and 68.22° appearing on the CaO poisoning catalyst surface, in which the peaks at 2θ = 36.79° and 68.22° (JCPDS 06-0540) corresponded to Mn₂O₃ and the peak at 2θ = 50.34° belonged to MnO₂ (JCPDS 42-1348). Moreover, the intensity of CeO₂ peak on CaO poisoning catalyst became stronger compared with Mn-Ce/AC. These results demonstrated that the crystallization and agglomeration phenomenon of the active components, especially manganese oxide, happened on the catalyst surface after doping CaO. More importantly, the peak of Mn₂O₃ could be detected on CaO poisoning catalyst surface, indicating that part of MnO₂ in AC surface was converted to Mn₂O₃. MnO₂ participated in a main catalytic role and promoted the conversion rate of NO to NO₂ [21,22]. The decrease of MnO₂ would definitely cause the reduction of the SCR performance for the catalyst.

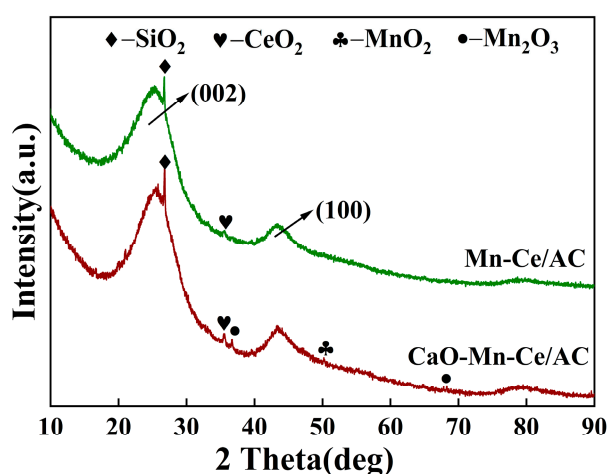


Figure 4. The XRD curves of the two catalysts.

2.5. XPS Analysis

The change of surface atomic on AC surface had an important influence on SCR reaction. Therefore, it was of great significance to discuss the change of the surface atomic structure of the catalyst.

The XPS spectra of Mn 2p for Mn-Ce/AC and CaO poisoning catalyst is displayed in Figure 5a. According to the reference [23,24], peaks of Mn 2p_{3/2} was divided into three peaks of 640.24, 642.15 and 646.60 eV, corresponding to Mn²⁺, Mn³⁺ and Mn⁴⁺, respectively. As shown in Figure 5a, the Mn⁴⁺ peak area of CaO poisoning catalyst decreased significantly. The valence ratios of Mn²⁺, Mn³⁺ and Mn⁴⁺ over Mn-Ce/AC were 30.99%, 34.29% and 34.72%, respectively. However, for CaO poisoning catalyst, the corresponding ratios were 29.52%, 44.05% and 26.43%. It was found that the content of Mn²⁺ did not change after loading CaO. Therefore, most of the reduced Mn⁴⁺ in AC surface was converted to Mn³⁺ after loading CaO. A similar conclusion was also obtained from XRD result (Figure 4). Mn⁴⁺ had the higher NO removal efficiency and redox ability compared with Mn³⁺ in the form of Mn₂O₃ [25,26]. Manganese dioxide also promoted the conversion of NO to NO₂ and the generation of active intermediate [22,27], which is beneficial to SCR reaction. So, loading CaO changed the manganese phase on AC surface and decreased the Mn⁴⁺ concentration.

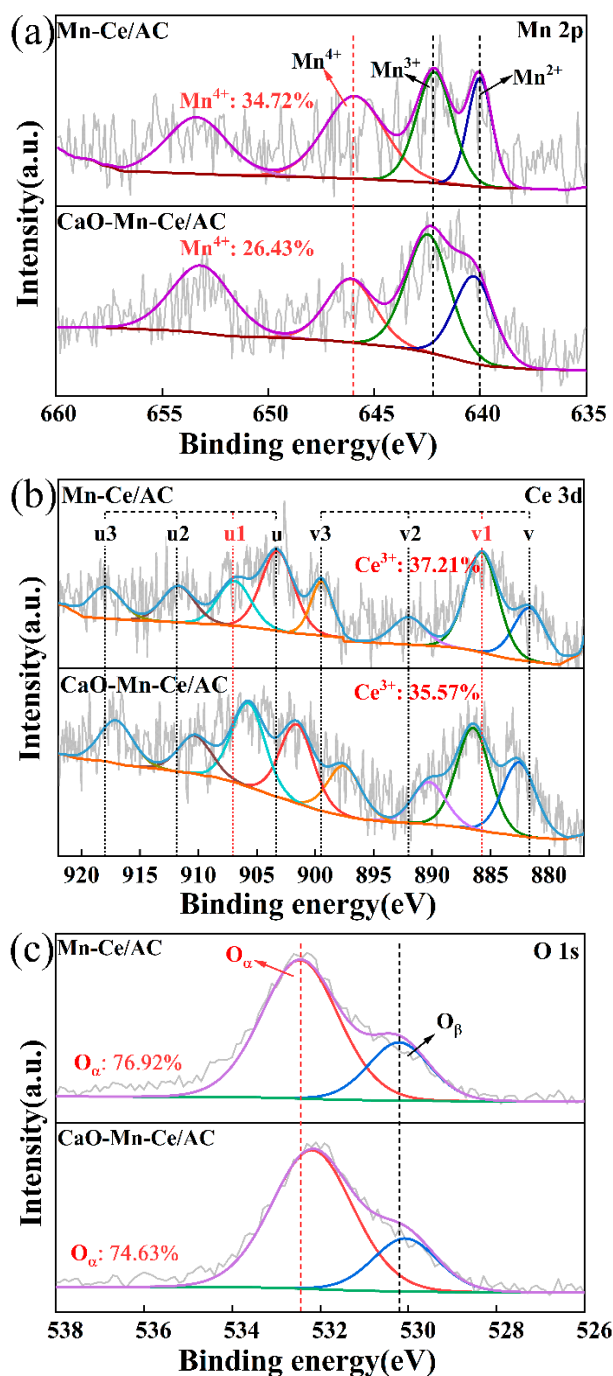


Figure 5. XPS spectra of (a) Mn 2p, (b) Ce 3d and (c) O 1s for the two catalysts.

XPS spectra of Ce 3d of the two catalysts are displayed Figure 5b. In these eight peaks, the peaks of u1 and v1 belonged to Ce^{3+} and the others were attributed to Ce^{4+} [16,28]. The reports [29,30] had suggested that Ce^{3+} was more conducive to the generation of oxygen vacancies and unsaturated chemical bonds. Therefore, the Ce^{3+} was favorable for SCR reaction. The Ce^{3+} and Ce^{4+} content of Mn-Ce/AC and CaO poisoning catalyst could be obtained from XPS spectra, and the ratio of Ce^{3+} for Mn-Ce/AC and CaO poisoning catalyst were 37.21% and 35.57%, respectively. Therefore, the content of Ce^{3+} only had a little change after loading CaO. So the valence of Ce was basically not affected by loading CaO.

The XPS of O 1s was consisted of two peaks at 532.4 eV and 530.2 eV, belonging to the chemisorption oxygen (O_α) and lattice oxygen (O_β), respectively [11,31]. From Figure 5c, the content of O_α for

Mn-Ce/AC catalyst was 76.92%, while that for CaO poisoning catalyst decreased to 74.63%. Similar to the XPS result of Ce, the ratio of O_{α} also had a little decrease after doping CaO. The amount of the chemisorption oxygen (O_{α}) was closely related to the valence of Ce [29], so loading CaO had almost no effect on the state of oxygen.

2.6. FT-IR Analysis

The FT-IR characterization was performed and the results are displayed in Figure 6. The FT-IR curves of both catalysts contained four bands at 1634, 3454, 1384 and 1080 cm^{-1} , which was corresponded to the stretching of C=O, the stretching vibrations of –OH groups, aliphatic C–H groups and C–O–C groups, respectively [32–35]. Studies have shown that –OH and C=O groups could provide adsorption sites for NH_3 and promote the transformation of ammonia gas ($\text{NH}_3(\text{g})$) to adsorbed ammonia ($\text{NH}_3(\text{ads})$) [10,36,37]. Besides, NH_3 and NO were more easily adsorbed when functional groups existed on the AC surface [33,37]. From Figure 6, the intensity of the bands at 1384 and 1080 cm^{-1} became weak. Moreover, the intensity of the bands at 3454 and 1634 cm^{-1} decreased obviously. This indicated that all oxygen-containing functional groups were reduced to some extent after doping CaO. Therefore, the presence of CaO destroyed the oxygen-containing functional groups and inhibited the SCR performance of the catalyst.

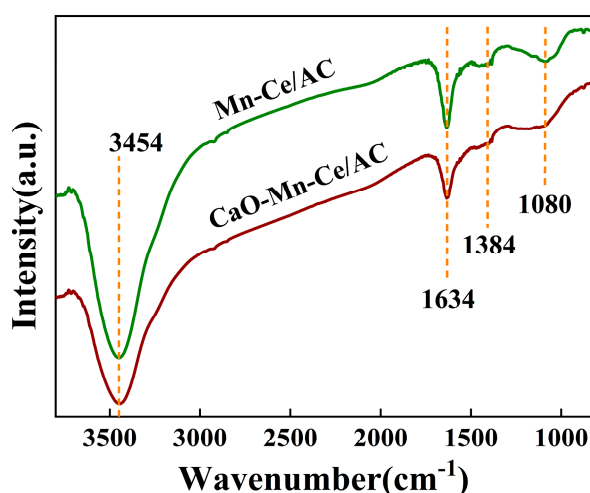


Figure 6. FT-IR spectra of the two catalysts.

2.7. Acidic Performance

Figure 7 showed NH_3 -TPD profiles of Mn-Ce/AC and CaO-Mn-Ce/AC catalysts. In NH_3 -TPD profiles, the acid amount and strength were decided by the area and position of the desorption peak [11]. From Figure 7, the peak of weak acid site on Mn-Ce/AC and CaO poisoning catalysts could be observed at about 130–170 $^{\circ}\text{C}$, which indicated that loading CaO did not change the position of the weak acid site. However, the peak intensity of weak acid site decreased after loading CaO. The peak of strong acid site on Mn-Ce/AC and CaO-Mn-Ce/AC catalysts could be observed at 614 $^{\circ}\text{C}$ and 819 $^{\circ}\text{C}$ and the peak of strong acid site on Mn-Ce/AC catalyst moved towards the higher temperature zone. Moreover, the peak area of strong acid site on Mn-Ce/AC catalyst became smaller after doping CaO. All the acid sites played an important role during the NO removal process and the higher the number of acid sites, the more NH_3 would be adsorbed on the surface of the catalyst [38]. Therefore, the decrease of weak and strong acid site was one of the factors for different SCR performance between Mn-Ce/AC and CaO poisoning catalysts.

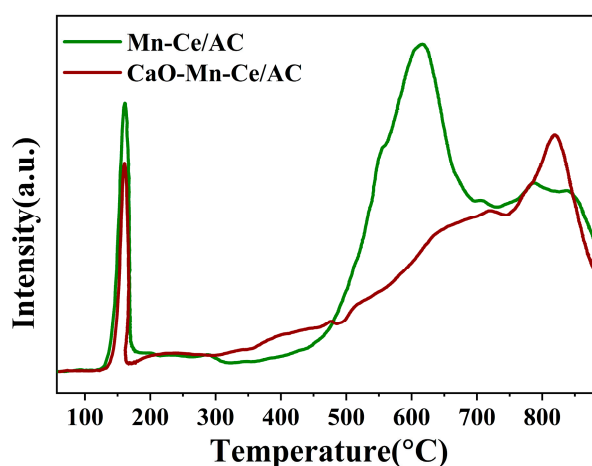
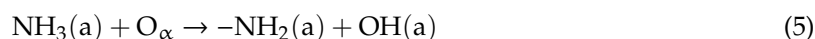
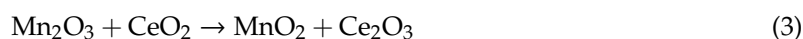


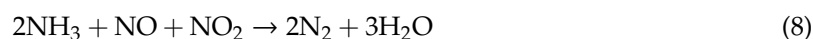
Figure 7. NH₃-TPD profiles of two catalysts.

3. Discussion

In our previous study [10], the Mn-Ce carbon-based catalyst has been studied and the NO removal reaction occurred on catalyst followed the Eley-Rideal (E-R) mechanism. The specific reaction steps are as follows:



Simultaneously, the “fast SCR” reaction would also occur on the Mn-Ce carbon-based catalyst [9]:



In the E-R mechanism, MnO₂ was reduced to Mn₂O₃ and provided the chemisorption oxygen (O_α) (Equation (2)) and it was a crucial step for the SCR reaction process. Besides, MnO₂ promoted the conversion rate of NO to NO₂ (Equation (7)) in the “fast SCR” reaction [9,22].

However, XRD and XPS results proved that part of MnO₂ in AC surface was converted to Mn₂O₃ in the process of loading CaO. Mn³⁺ in the form of Mn₂O₃ had the lower redox ability compared with MnO₂. Therefore, the decrease of MnO₂ resulted in a decline of generation rate for the chemisorption oxygen and inhibited the formation of intermediate product -NH₂ (Shown in Figure 8). Furthermore, the decrease of MnO₂ also caused the reduction of reaction rate for the “fast SCR” reaction (Figure 8) because of less NO₂ production (Equation (7)). Therefore, the change of manganese oxide form inhibited generation rate for the chemisorption oxygen and NO₂, which was the most critical reason for the decrease of catalytic activity for Mn-Ce/AC catalyst.

The intensity of all bands for functional groups decreased after loading CaO (from FT-IR result), indicating the oxygen-containing functional groups of CaO poisoning catalyst were destroyed (From Figure 6). The decrease of oxygen-containing functional groups, especially -OH and C=O groups, resulted in the less gas being absorbed onto the AC surface (Shown in Figure 8). This was the limiting factor for increasing the reaction rate of the NO removal process. The decrease of weak and strong

acid site also hindered the adsorption of NH_3 . In addition, CaO also caused the reduction of the BET surface area and total pore volume of the catalyst (from Figure 3). The large BET surface area could provide more contact opportunities for adsorbed gas (NH_3 and NO) and active components. So the oxygen-containing functional groups and the reduction of BET surface area was also one of the reasons for the deactivation of Mn-Ce/AC catalyst.

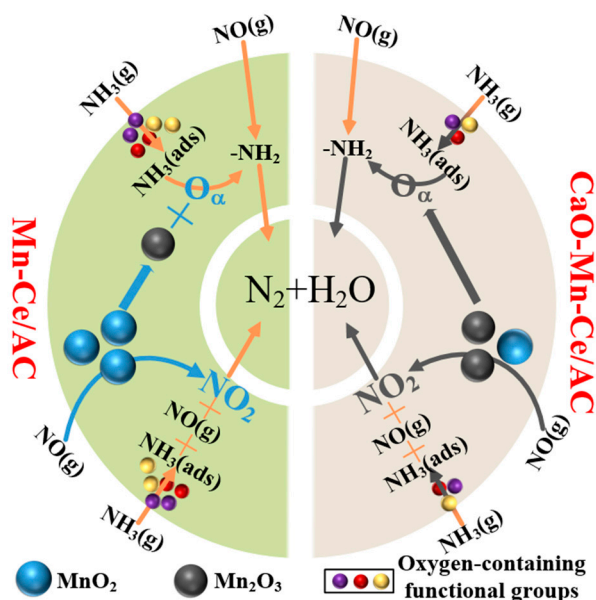


Figure 8. Poisoning effect of CaO on SCR reaction for Mn-Ce/AC catalyst.

4. Materials and Methods

4.1. Catalyst Preparation

The AC carrier was provided by Shanxi Xin-Hua Activated Carbon Factory and the particle size of AC used in this experiment was 16–20 mesh. First, it was pretreated with 65 wt% HNO_3 solution at 80°C for 8 h. Finally, the pretreated AC was dried at 120°C for 10 h.

The precursors used in the experiment were 50 wt% $\text{Mn}(\text{NO}_3)_2$, $\text{Ce}(\text{NO}_3)_3 \cdot 6\text{H}_2\text{O}$ and $\text{Ca}(\text{NO}_3)_2$. Active components Mn and Ce were supported onto the surface of the AC by impregnation method. The total weight percentage of CeO_2 and MnO_2 loading was 10% (Mn/Ce (molar ratio) = 7:3). First, AC was immersed in the prepared precursors, followed by ultrasonic Oscillation for 30 min, then placing in the water bath at 65°C for 12 h. Finally, the mixture was calcined at 400°C for 4 h. The obtained catalyst was marked as Mn-Ce/AC . The CaO poisoning catalysts were prepared by impregnating $\text{Ca}(\text{NO}_3)_2$ onto fresh catalyst, and molar ratios of Ca/Mn were 0.5. The samples obtained were marked as CaO-Mn-Ce/AC .

4.2. Catalytic Activity Measurements

The mass of the catalyst sample using in the experiments was 1 g. The flow rate was 500 mL/min with 500 ppm NO and NH_3 , 5% O_2 , and N_2 as the balance gas. The temperature range was from 75°C to 250°C and a flue gas analyzer was used to monitored continuously the outlet gas concentrations of NO . The catalytic activity was calculated by the formulas:

$$\text{NO conversion (\%)} = \frac{[\text{NO}]_{\text{in}} - [\text{NO}]_{\text{out}}}{[\text{NO}]_{\text{in}}} \times 100\% \quad (9)$$

$$\text{N}_2 \text{ selectivity} = \left(1 - \frac{2 \times [\text{N}_2\text{O}]_{\text{out}}}{[\text{NO}_x]_{\text{in}} + [\text{NH}_3]_{\text{in}} - [\text{NO}_x]_{\text{out}} - [\text{NH}_3]_{\text{out}}} \right) \times 100\% \quad (10)$$

4.3. Catalyst Characterization

Nitrogen adsorption isotherm was measured with Micromeritics ASAP 2010 instrument at 77 K. The BET and the t-plot method were used to calculate the BET specific surface, the total pore volume and average pore size. The microstructures of the experimental samples were studied by Scanning Electron Micrograph (SEM, JEOL S-4800). XRD was operated by Rigaku D/max-2500/PC diffractometer with the scanning range of 10 to 90°. X-ray photoelectron spectra (XPS) were obtained with Al K α X-ray ($h\nu = 1486.6$ eV) radiation at 150 W from Thermo Scientific ESCALAB 250. Nicolet 5DXC spectrometer was used to record Fourier Transform Infrared Spectroscopy (FT-IR) and investigate the surface functional groups of catalysts in the range of 4000–400 cm⁻¹.

5. Conclusions

Mn-Ce/AC and CaO poisoning catalysts were prepared by the impregnation method and the poisoning effect of CaO on the catalyst was discussed in this study. The activity test experiment showed that loading CaO inhibited the catalytic activity of Mn-Ce/AC catalyst and the NO conversion of the catalyst decreased from 69.5% to the 38.2% at 75 °C. CaO poisoning catalyst had the smaller N₂ selectivity compared with Mn-Ce/AC catalyst. MnO₂ played a main catalytic role on SCR reaction and promoted the conversion rate of NO to NO₂. However, the amount of MnO₂ in AC surface decreased in the process of loading CaO, which was detrimental to the SCR performance of the catalyst. The change of manganese oxide form inhibited generation rate for the chemisorption oxygen and NO₂, which was the most critical reason for the decrease of catalytic activity for Mn-Ce/AC. In addition, loaded CaO entered into the pores of the catalyst, which led to the blockage of the pores and further led to the decrease of the BET surface area and total pore volume. It also destroyed the oxygen-containing functional groups of CaO poisoning catalyst. All of these caused the decrease of SCR activity for Mn-Ce/AC catalyst after loading CaO.

Author Contributions: Conceptualization, S.R. and Z.S.; methodology, Z.S.; validation, S.R., Z.S. and Z.C.; formal analysis, J.Y.; investigation, J.Y.; data curation, Z.C. and Y.Z.; writing—original draft preparation, Z.S.; writing—review and editing, S.R., L.J. and C.Y.; funding acquisition, S.R. All authors have read and agreed to the published version of the manuscript.

Funding: This research was funded by National Natural Science Foundation of China, grant number No. 51874058 and Fund of Chongqing Science and Technology, grant number CQYC201905017 and cstc2019jcsx-msxmX0215.

Conflicts of Interest: The authors declare no conflict of interest.

References

1. Ren, S.; Li, S.; Su, Z.; Yang, J.; Long, H.; Kong, M.; Yang, J.; Cai, Z. Poisoning effects of KCl and As₂O₃ on selective catalytic reduction of NO with NH₃ over Mn-Ce/AC catalysts at low temperature. *Chem. Eng. J.* **2018**, *351*, 540–547. [[CrossRef](#)]
2. Lu, X.; Song, C.; Chang, C.; Teng, Y.; Tong, Z.; Tang, X. Manganese oxides supported on TiO₂-graphene nanocomposite catalysts for selective catalytic reduction of NO_x with NH₃ at low temperature. *Ind. Eng. Chem. Res.* **2014**, *53*, 11601–11610. [[CrossRef](#)]
3. Xie, X.; Lu, J.; Hums, E.; Huang, Q.; Lu, Z. Study on the deactivation of V₂O₅-WO₃/TiO₂ selective catalytic reduction catalysts through transient kinetics. *Energy Fuels* **2015**, *29*, 3890–3896. [[CrossRef](#)]
4. Zhu, L.; Huang, B.; Wang, W.; Wei, Z.; Ye, D. Low-temperature SCR of NO with NH₃ over CeO₂ supported on modified activated carbon fibers. *Catal. Commun.* **2011**, *12*, 394–398. [[CrossRef](#)]
5. He, H.; Yu, Y. Selective catalytic reduction of NO. *Catal. Today* **2005**, *100*, 37–47. [[CrossRef](#)]
6. Grzybek, T.; Klinik, J.; Motak, M.; Papp, H. Nitrogen-promoted active carbons as catalytic supports: 2. The influence of Mn promotion on the structure and catalytic properties in SCR. *Catal. Today* **2008**, *137*, 235–241. [[CrossRef](#)]
7. Samojeden, B.; Grzybek, T. The influence of the promotion of N-modified activated carbon with iron on NO removal by NH₃-SCR (Selective catalytic reduction). *Energy* **2016**, *116*, 1484–1491. [[CrossRef](#)]

8. Marban, G.; Fuertes, A.B. Low-temperature SCR of NO_x with NH₃ over Nomex™ rejects-based activated carbon fibre composite-supported manganese oxides: Part I. Effect of pre-conditioning of the carbonaceous support. *Appl. Catal. B Environ.* **2001**, *34*, 43–53. [[CrossRef](#)]
9. Ren, S.; Yang, J.; Zhang, T.; Jiang, L.; Long, H.; Guo, F.; Kong, M. Role of cerium in improving NO reduction with NH₃ over Mn-Ce/ASC catalyst in low-temperature flue gas. *Chem. Eng. Res. Des.* **2018**, *133*, 1–10. [[CrossRef](#)]
10. Yang, J.; Su, Z.; Ren, S.; Long, H.; Kong, M.; Jiang, L. Low-temperature SCR of NO with NH₃ over biomass char supported highly dispersed Mn-Ce mixed oxides. *J. Energy Inst.* **2019**, *92*, 883–891. [[CrossRef](#)]
11. Yang, J.; Ren, S.; Zhang, T.; Su, Z.; Long, H.; Kong, M.; Yao, L. Iron doped effects on active sites formation over activated carbon supported Mn-Ce oxide catalysts for low-temperature SCR of NO. *Chem. Eng. J.* **2020**, *379*, 122398. [[CrossRef](#)]
12. Jiang, L.J.; Liu, Q.C.; Zhao, Q.; Ren, S.; Kong, M.; Yao, L.; Meng, F. Promotional effect of Ce on the SCR of NO with NH₃ at low temperature over MnO_x supported by nitric acid-modified activated carbon. *Res. Chem. Intermed.* **2018**, *44*, 1729–1744. [[CrossRef](#)]
13. Su, Z.; Ren, S.; Zhang, T.; Yang, J.; Zhou, Y.; Yao, L. Effects of PbO poisoning on Ce-Mn/AC catalyst for low-temperature selective catalytic reduction of NO with NH₃. *J. Iron Steel Res. Int.* **2020**. [[CrossRef](#)]
14. Li, X.; Liu, C.; Li, X.; Peng, Y.; Li, J. A neutral and coordination regeneration method of Ca-poisoned V₂O₅-WO₃/TiO₂ SCR catalyst. *Catal. Commun.* **2017**, *100*, 112–116. [[CrossRef](#)]
15. Wang, X.; Zhou, J.; Wang, J.; Ding, A.; Gui, K.; Thomas, H. The effect of different Ca precursors on the activity of manganese and cerium oxides supported on TiO₂ for NO abatement. *React. Kinet. Mech. Catal.* **2020**, *129*, 153–164. [[CrossRef](#)]
16. Liu, S.; Guo, R.; Wang, S.; Pan, W.; Sun, P.; Li, M.; Liu, S. Deactivation mechanism of Ca on Ce/TiO₂ catalyst for selective catalytic reduction of NO_x with NH₃. *J. Taiwan Inst. Chem. Eng.* **2017**, *78*, 290–298. [[CrossRef](#)]
17. Zhou, J.; Wang, X.; He, X.; Wang, J.; Gui, K.; Thomas, H. The effect of SO₂ and Ca Co-pretreatment on the catalytic activity of Mn–Ce/TiO₂ catalysts for selective catalytic reduction of NO with NH₃. *Catal. Lett.* **2020**. [[CrossRef](#)]
18. Lu, L.; Sahajwalla, V.; Kong, C.; Harris, D. Quantitative X-ray diffraction analysis and its application to various coals. *Carbon* **2001**, *39*, 1821–1833. [[CrossRef](#)]
19. Orimo, S.; Matsushima, T.; Fujii, H.; Fukunaga, T.; Majer, G. Hydrogen desorption property of mechanically prepared nanostructured graphite. *J. Appl. Phys.* **2001**, *90*, 1545–1549. [[CrossRef](#)]
20. Chen, X.; Wang, P.; Fang, P.; Ren, T.; Liu, Y.; Cen, C.; Wang, H.; Wu, Z. Tuning the property of Mn-Ce composite oxides by titanate nanotubes to improve the activity, selectivity and SO₂/H₂O tolerance in middle temperature NH₃-SCR reaction. *Fuel Process. Technol.* **2017**, *167*, 221–228. [[CrossRef](#)]
21. Wu, W.; Zeng, Z.; Lu, P.; Xing, Y.; Wei, J.; Yue, H.; Li, R. Simultaneous oxidation of Hg⁰ and NH₃-SCR of NO by nanophase Ce_xZr_yMn_zO₂ at low temperature: The interaction and mechanism. *Environ. Sci. Pollut. Res.* **2018**, *25*, 14471–14485. [[CrossRef](#)] [[PubMed](#)]
22. Zhou, L.; Li, C.; Zhao, L.; Zeng, G.; Gao, L.; Wang, Y.; Yu, M. The poisoning effect of PbO on Mn-Ce/TiO₂ catalyst for selective catalytic reduction of NO with NH₃ at low temperature. *Appl. Surf. Sci.* **2016**, *389*, 532–539. [[CrossRef](#)]
23. Zhao, B.; Ran, R.; Guo, X.; Cao, L.; Xu, T.; Chen, Z.; Wu, X.; Si, Z.; Weng, D. Nb-modified Mn/Ce/Ti catalyst for the selective catalytic reduction of NO with NH₃ at low temperature. *Appl. Catal. A Gen.* **2017**, *545*, 64–71. [[CrossRef](#)]
24. Wu, Z.; Jin, R.; Liu, Y.; Wang, H. Ceria modified MnO_x/TiO₂ as a superior catalyst for NO reduction with NH₃ at low-temperature. *Catal. Commun.* **2008**, *9*, 2217–2220. [[CrossRef](#)]
25. Thirupathi, B.; Smirniotis, P. Nickel-doped Mn/TiO₂ as an efficient catalyst for the low-temperature SCR of NO with NH₃: Catalytic evaluation and characterizations. *J. Catal.* **2012**, *288*, 74–83. [[CrossRef](#)]
26. Kang, M.; Park, E.; Kim, J.; Yie, J. Manganese oxide catalysts for NO_x reduction with NH₃ at low temperatures. *Appl. Catal. A Gen.* **2007**, *327*, 261–269. [[CrossRef](#)]
27. Cimino, S.; Totarella, G.; Tortorelli, M.; Lisi, L. Combined poisoning effect of K⁺ and its counter-ion (Cl⁻ or NO₃⁻) on MnO_x/TiO₂ catalyst during the low temperature NH₃-SCR of NO. *Chem. Eng. J.* **2017**, *330*, 92–101. [[CrossRef](#)]

28. Zhang, X.; Wang, J.; Song, Z.; Zhao, H.; Xing, Y.; Zhao, M.; Zhao, J.; Ma, Z.; Zhang, P.; Tsubaki, N. Promotion of surface acidity and surface species of doped Fe and SO_4^{2-} over CeO_2 catalytic for NH_3 -SCR reaction. *Mol. Catal.* **2019**, *463*, 1–7. [[CrossRef](#)]
29. Lee, K.; Kumar, P.; Maqbool, M.; Rao, K.; Song, K.; Ha, H. Ceria added Sb- $\text{V}_2\text{O}_5/\text{TiO}_2$ catalysts for low temperature NH_3 SCR: Physico-chemical properties and catalytic activity. *Appl. Catal. B Environ.* **2013**, *142–143*, 705–717. [[CrossRef](#)]
30. Chen, L.; Li, J.; Ge, M.; Zhu, R. Enhanced activity of tungsten modified $\text{CeO}_2/\text{TiO}_2$ for selective catalytic reduction of NO_x with ammonia. *Catal. Today* **2010**, *153*, 77–83. [[CrossRef](#)]
31. Niu, Y.; Shang, T.; Hui, S.; Zhang, X.; Lei, Y.; Lv, Y.; Wang, S. Synergistic removal of NO and N_2O in low-temperature SCR process with MnO_x/Ti based catalyst doped with Ce and V. *Fuel* **2016**, *185*, 316–322. [[CrossRef](#)]
32. Zhang, L.; Cui, S.; Guo, H.; Ma, X.; Luo, X. The influence of K^+ cation on the $\text{MnO}_x\text{-CeO}_2/\text{TiO}_2$ catalysts for selective catalytic reduction of NO_x with NH_3 at low temperature. *J. Mol. Catal. A Chem.* **2014**, *390*, 14–21. [[CrossRef](#)]
33. He, H.; Dai, H.; Au, C. Defective structure, oxygen mobility, oxygen storage capacity, and redox properties of RE-based (RE=Ce, Pr) solid solutions. *Catal. Today* **2004**, *90*, 245–254. [[CrossRef](#)]
34. Qu, L.; Li, C.; Zeng, G.; Zhang, M.; Fu, M.; Ma, J.; Zhan, F.; Luo, D. Support modification for improving the performance of $\text{MnO}_x\text{-CeO}_y/\gamma\text{-Al}_2\text{O}_3$ in selective catalytic reduction of NO by NH_3 . *Chem. Eng. J.* **2014**, *242*, 76–85. [[CrossRef](#)]
35. Yang, S.; Liao, Y.; Xiong, S.; Qi, F.; Dang, H.; Xiao, X.; Li, J. N_2 selectivity of NO reduction by NH_3 over $\text{MnO}_x\text{-CeO}_2$: Mechanism and key factors. *J. Phys. Chem. C* **2014**, *118*, 21500–21508. [[CrossRef](#)]
36. Teng, H.; Tu, Y.; Lai, Y.; Lin, C. Reduction of NO with NH_3 over carbon catalysts: The effects of treating carbon with H_2SO_4 and HNO_3 . *Carbon* **2001**, *39*, 575–582. [[CrossRef](#)]
37. Guo, Q.; Jing, W.; Hou, Y.; Huang, Z.; Ma, Z.; Han, X.; Sun, D. On the nature of oxygen groups for NH_3 -SCR of NO over carbon at low temperatures. *Chem. Eng. J.* **2015**, *270*, 41–49. [[CrossRef](#)]
38. Fan, Z.; Shi, J.; Niu, C.; Wang, B.; He, C.; Cheng, Y. The insight into the role of Al_2O_3 in promoting the SO_2 tolerance of MnO_x for low-temperature selective catalytic reduction of NO_x with NH_3 . *Chem. Eng. J.* **2020**, *398*, 125572. [[CrossRef](#)]

